

Switchable mirrors based on nickel–magnesium films

T. J. Richardson,^{a)} J. L. Slack, R. D. Armitage, R. Kostecki, B. Farangis, and M. D. Rubin
Environmental Energy Technologies Division, Lawrence Berkeley National Laboratory, Berkeley, California 94720

(Received 23 January 2001; accepted for publication 20 March 2001)

An electrochromic mirror electrode based on reversible uptake of hydrogen in nickel magnesium alloy films is reported. Thin, magnesium-rich Ni–Mg films prepared on glass substrates by co-sputtering from Ni and Mg targets are mirror-like in appearance and have low visible transmittance. Upon exposure to hydrogen gas or on cathodic polarization in alkaline electrolyte, the films take up hydrogen and become transparent. When hydrogen is removed, the mirror properties are recovered. The transition is believed to result from reversible formation of Mg_2NiH_4 and MgH_2 . A thin overlayer of palladium was found to enhance the kinetics of hydrogen insertion and extraction, and to protect the metal surface against oxidation. © 2001 American Institute of Physics. [DOI: 10.1063/1.1371959]

Devices capable of switching between mirror and transparent states may find applications in architectural and transportation energy conservation, lighting and displays, aerospace insulation control, and optical communications systems. Switchable mirrors based on rare earth hydrides were discovered by Huiberts *et al.*,¹ who observed a reversible metal-to-insulator transition when a thin film (150 to 500 nm) of yttrium or lanthanum coated with a thin layer of palladium was exposed to hydrogen gas. The transition accompanies conversion of a metallic dihydride phase to a semiconducting trihydride. Rare earth-magnesium alloy films² were subsequently found to be superior to the pure lanthanides in maximum transparency and mirror-state reflectivity. Phase separation appears to occur when these alloys take up hydrogen, giving transparent MgH_2 and LnH_{2-3} , both of which may participate in the switching mechanism.³ Because the rare earths are highly vulnerable to oxidation, a Pd overlayer at least 5 nm thick is required for films exposed to air or to an alkaline electrolyte. Although the Pd catalyzes the uptake and removal of hydrogen, it limits the maximum transparency of the composite film to about 50%.⁴ The influence of the Pd layer and of a Pd/ AlO_x composite cap layer on hydrogen uptake by rare earth-based films have been studied extensively by van Gogh *et al.*⁵ and by van der Molen *et al.*⁶

Among the many transition metals and alloys that have been investigated for use in low pressure hydrogen storage devices or as electrodes in secondary batteries, a few are known to form semiconducting hydride phases such as Mg_2NiH_4 ,⁷ Mg_2CoH_5 ,⁸ and Mg_2FeH_6 .⁹ In the case of nickel, a stoichiometric alloy phase, Mg_2Ni , with the same Mg–Ni ratio as in the hydride, can be prepared from the elements. In Mg_2Ni [Fig. 1(a)], there are Ni–Ni bonds (shown as hollow rods), two types of Ni–Mg bonds (solid rods) and three types of Mg–Mg bonds (not shown).¹⁰ The Ni–Ni bonds and Mg–Mg bonds are shorter in the alloy than in the pure elements. The alloy absorbs hydrogen without structural rearrangement up to a composition of $\text{Mg}_2\text{NiH}_{0.3}$.⁷ This phase

has metallic properties similar to those of the pure alloy. Further introduction of hydrogen produces Mg_2NiH_4 [Fig. 1(b)]. In this material,¹¹ each nickel atom is surrounded by four hydrogen atoms in a tetrahedral array, with short Ni–H bond lengths and Mg–H bonds slightly longer than those in magnesium hydride (MgH_2).¹² No Ni–Mg bonds remain. Mg_2NiH_4 is a red solid.⁷ Its optical band gap has been reported variously as 2.0,¹³ 1.9,¹⁴ and 1.7¹⁵ eV for bulk samples, and 1.3 eV for an Ni–Mg–H film of unknown composition.¹⁶ MgH_2 is a colorless insulator, $E_g = 5.16$ eV.¹⁷ Although the bulk hydrides are generally prepared at elevated temperature and pressure, the H_2 dissociation pressures at 25 °C are ca. 1×10^{-5} atm for Mg_2NiH_4 ⁷ and 1×10^{-6} atm for MgH_2 .¹⁸

Ni–Mg films were deposited by dc magnetron co-sputtering from 2 in diameter Ni and Mg (99.98%) targets onto glass substrates with and without transparent conductive coatings. The base pressure was 1.4×10^{-7} Torr, process pressure 2 mTorr, Ni power 20 W, Mg power 22 W, and target-to-substrate distance 7.5 cm. Deposition rates ranged from 0.33 to 0.55 nm/s, depending on location of the substrate in the horizontal plane over the sputter sources. When used, the Pd over-layer was applied at 10 mTorr, Pd power 12.4 W, and deposition rate 0.16 nm/s. Film thicknesses were measured by stylus profilometry. Samples for mid-IR

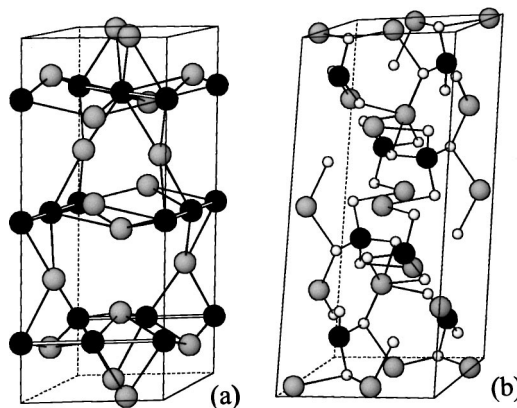


FIG. 1. Crystal structures of (a) Mg_2Ni and (b) Mg_2NiH_4 . Large black spheres: Ni, large gray spheres: Mg, small spheres H.

^{a)}Electronic mail: tjrichardson@lbl.gov

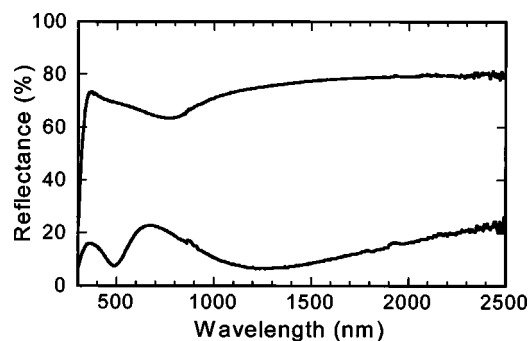


FIG. 2. Reflectance spectra of 80 nm Ni-Mg film with 5 nm Pd overlayer on glass substrate in the metallic (upper curve) and hydride (lower curve) states. Spectra were recorded from the back (substrate) side.

spectroscopy were deposited on high-resistivity silicon discs and measured by reflectance at 45° through the silicon substrates. Samples for Raman spectroscopy were prepared on 0.1 mm thick glass to minimize substrate contributions to the spectra.

Switching from the as-deposited mirror state to the transparent state was achieved by exposing the films to a dry gas stream containing 4% hydrogen in argon or helium. The mirror state was recovered by exposing the films to ambient air. Electrochemical switching was carried out in aqueous alkaline electrolyte (5–8 M KOH, Pt counter electrode, HgO/Hg reference), with *in situ* measurement of optical transmission spectra or photopic transmittance. Film compositions were determined by Rutherford backscattering spectrometry (RBS) and particle induced x-ray emission (PIXE).

The freshly deposited Ni-Mg films were amorphous by x-ray diffraction (XRD) showing only weak reflections due to Pd. After annealing in dry nitrogen at 125°C , Mg_2Ni , Mg, and Mg_6Pd were present. The annealed films did not take up hydrogen readily, and no changes were observed in the XRD pattern obtained under a stream of 4% H_2 . All Ni-Mg films were highly reflective (Fig. 2) and had very low transmittance (Fig. 3). The transition speed and maximum transmittance depended upon the Ni to Mg ratio (see below). Films without a Pd overlayer switched very slowly and less completely. Gasochromic switching times of less than 10 s were achieved. Co-sputtering from offset sources produced films with position-dependent Ni-Mg atomic ratios. RBS-PIXE analysis showed that areas with Mg:Ni atomic ratios between 4.5:1 and 7:1 became transparent on the first exposure to H_2 . On subsequent hydriding following air oxidation, the area of switching expanded to include Mg:Ni ratios from 3.5:1 to

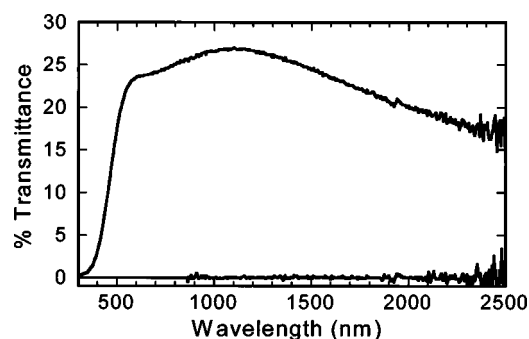


FIG. 3. Transmittance spectra of 80 nm Ni-Mg film with 5 nm Pd overlayer on glass substrate in metallic (lower curve) and hydride (upper curve) states.

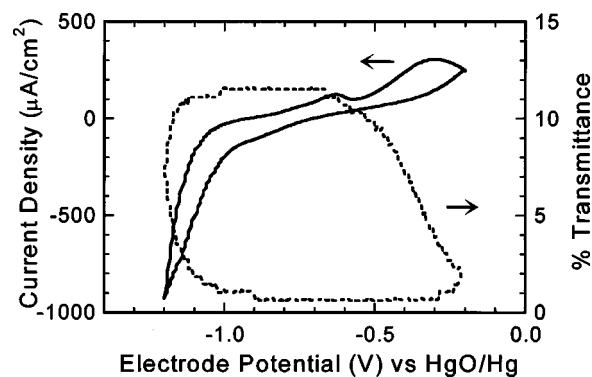


FIG. 4. Electrochemical switching (cycle number 4 shown, others are similar) of 50 nm Ni-Mg film with 10 nm Pd overlayer on ITO glass. Scan rate: 5 mV/s, active area: 5.0 cm^2 .

10:1. The color of thick transparent films varied from pale yellow in Mg-rich regions to deep red in Ni-rich areas. The absorption edge of Mg_2NiH_4 is shifted to shorter wavelengths by the presence of MgH_2 as in the case of rare earth-Mg hydride mixtures.² The estimated optical band gap varied from 2.8 eV for films containing a large excess of Mg, to about 2.5 eV for Mg:Ni \approx 4.

Electrochemical hydrogen loading produced similar switching between mirror and transparent states (Fig. 4). Only a broad reduction feature beginning at -0.8 V , accompanied by a small increase in transmittance is observed before the onset of hydrogen evolution at around -1.0 V , when the film rapidly becomes clear. A small anodic peak centered at -0.6 V , and probably due to hydrogen desorption from the Pd overlayer, signals the onset of the return to the metallic state, a somewhat slower process than hydrogen uptake. The anodic current peaks at -0.3 V , with complete recovery of the mirror-like appearance. The charge passed during the anodic sweep is 61 mC/cm^2 . The theoretical capacities of Mg and Mg_2Ni are 1.38 and 1.24 mC/nm^2 . Since the Pd layer can account for no more than about 10 mC/cm^2 , the Ni-Mg capacity is that expected for a 37 to 41 nm thickness, depending on Ni-Mg ratio, consistent with the measured thickness of 50 nm and allowing for some porosity. Switching to the clear state in 40 s and to the mirror state in 90 s could be achieved by stepping the potential to -1.2 and -0.2 V , respectively.

The presence of Mg_2NiH_4 in the transparent films is supported by vibrational spectroscopy (Fig. 5). The Raman peak at about 1650 cm^{-1} and the infrared absorption maximum at 1600 cm^{-1} are attributed to ν_1 and ν_3 of the tetrahedral NiH_4^{4-} unit. While all four vibrational modes of a regular tetrahedron are Raman active, the symmetric stretching mode, ν_1 , generally has the highest intensity, and is similar in frequency to the stronger of the two IR absorption modes, ν_3 . No Raman spectrum has been reported for Mg_2NiH_4 . In the isoelectronic species, AsH_4^+ and GaH_4^- , ν_1 appears at 2080 and 1807 cm^{-1} , respectively.¹⁹ The stretching frequencies decrease with decreasing charge on the central atom (zero in the case of NiH_4^{4-}) and are lowered by hydrogen bonding,¹⁹ which is pronounced in Mg_2NiH_4 . An infrared absorption at 1638 cm^{-1} has been reported for bulk Mg_2NiH_4 .²⁰ The other prominent feature in the infrared spectrum of the hydrided film is a broad absorption centered

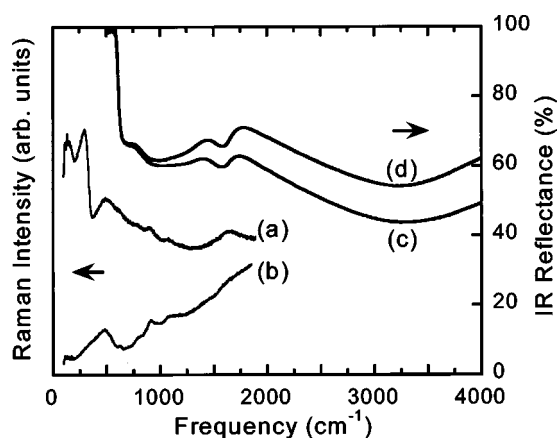


FIG. 5. Raman spectra of: (a) $1\text{ }\mu\text{m}$ Ni-Mg film on glass in hydride state, obtained from substrate side, and (b) of glass substrate, IR internal reflectance spectra of (c) $1\text{ }\mu\text{m}$ Ni-Mg film on Si in hydride state and (d) as (c) but with higher Mg/Ni ratio.

around 1000 cm^{-1} . This peak is relatively stronger than that of Mg_2NiH_4 (the baseline also varies with Ni:Mg ratio) in regions of the film with higher Mg content [Fig. 5(d)], and is assigned to MgH_2 .²¹ All absorption features disappear when hydrogen is removed from the film, and reappear when it is loaded again with hydrogen.

Hydrogen uptake by pure Mg is slow at ambient temperature and is kinetically hindered by formation of a dense surface layer of MgH_2 .^{22,23} The rate is increased by the presence of nickel^{24,25} or oxide²⁶ on the Mg surface, or by decreased crystallinity.²⁷ We observed faster switching in film areas with higher nickel content, and gradual improvement with time and switching cycle, especially in the more Mg-rich regions. The latter may be due to alloying of unreacted Ni and Mg, or to surface oxidation caused by a disruption of the Pd coating during cycling. Since no transparent binary hydride of nickel is known, it is clear that a nickel magnesium hydride (Mg_2NiH_4) must participate in the switching phenomenon. Formation of Mg_2NiH_4 or MgH_2 from their metallic precursors results in a volume increase of about 32% in each case. Ni-Mg films on thin glass substrates exhibited significant bending on exposure to hydrogen, while a $1.2\text{ }\mu\text{m}$ thick film confined on a rigid substrate was found by profilometry to increase in thickness by 31%. Preliminary results indicate similar switching behavior in cobalt-magnesium films.

In conclusion, a class of switchable mirror based on a transition metal alloy film has been discovered. The rapid, reversible conversion from the highly reflecting metallic state to a transparent semiconducting state is due to forma-

tion of known metal hydride phases, and can be produced by either electrochromic or gasochromic means.

The authors thank Dr. Kin Man Yu of LBNL, for performing RBS and PIXE measurements. This work was supported by the Assistant Secretary for Energy Efficiency and Renewable Energy, Office of Building Technologies, Building Systems and Materials Division of the US Department of Energy under Contract No. DE-AC03-76SF00098.

- ¹J. N. Huiberts, R. Griessen, J. H. Rector, R. J. Wijngaarden, J. P. Dekker, D. G. de Groot, and N. J. Koeman, *Nature (London)* **380**, 231 (1996).
- ²P. van der Sluis, M. Ouwerkerk, and P. A. Duine, *Appl. Phys. Lett.* **70**, 3356 (1997).
- ³D. G. Nagengast, A. T. M. van Gogh, E. S. Kooij, B. Dam, and R. Griessen, *Appl. Phys. Lett.* **75**, 2050 (1999).
- ⁴K. von Rottkay, M. Rubin, and P. A. Duine, *J. Appl. Phys.* **85**, 408 (1999).
- ⁵A. T. M. van Gogh, S. J. van der Molen, J. W. J. Kerssemakers, N. J. Koeman, and R. Griessen, *Appl. Phys. Lett.* **77**, 815 (2000).
- ⁶S. J. van der Molen, J. W. J. Kerssemakers, J. H. Rector, N. J. Koeman, B. Dam, and R. Griessen, *J. Appl. Phys.* **86**, 6107 (1999).
- ⁷J. J. Reilly and R. H. Wiswall, *Inorg. Chem.* **7**, 2254 (1968).
- ⁸P. Zolliker, K. Yvon, P. Fischer, and J. Schefer, *Inorg. Chem.* **24**, 4177 (1985).
- ⁹J. J. Didisheim, P. Zolliker, K. Yvon, P. Fischer, J. Schefer, and M. Gubelmann, *Inorg. Chem.* **23**, 1953 (1984).
- ¹⁰D. Noreus and P. E. Werner, *Acta Chem. Scand., Ser. A* **36**, 847 (1982).
- ¹¹P. Zolliker, K. Yvon, J. D. Jorgensen, and F. J. Rotella, *Inorg. Chem.* **25**, 3590 (1986).
- ¹²W. H. Zachariasen, C. E. Holley, and J. F. Stamper, *Acta Crystallogr.* **16**, 352 (1963).
- ¹³P. Selvam, B. Wiswanathan, and V. Srinivasan, *J. Electron Spectrosc. Relat. Phenom.* **46**, 357 (1988).
- ¹⁴D. Lupu, R. Grecu, and S. I. Farcas, *Z. Phys. Chem. (Munich)* **181**, 143 (1993).
- ¹⁵D. Lupu, R. Sarbu, and A. Biris, *Int. J. Hydrogen Energy* **12**, 425 (1987).
- ¹⁶Y. Fujita, M. Yamaguchi, and I. Yamamoto, *Z. Phys. Chem. (Munich)* **163**, 633 (1989).
- ¹⁷G. Krasko, in *Metal-Hydrogen Systems*, edited by T. Nejat Veziroglu (Pergamon, New York, 1982), p. 367.
- ¹⁸B. Bogdanović, *Int. J. Hydrogen Energy* **9**, 937 (1984).
- ¹⁹K. Nakamoto, *Infrared and Raman Spectra of Inorganic and Coordination Compounds*, 4th ed. (Wiley, New York, 1986), pp. 130–131.
- ²⁰N. Huang, H. Yamauchi, J. Wu, and Q. Wang, *Z. Phys. Chem. (Munich)* **163**, 225 (1989).
- ²¹J. R. Santisteban, G. J. Cuello, J. Davidowski, A. Fainstein, H. A. Peretti, A. Ivanov, and F. J. Bermejo, *Phys. Rev. B* **62**, 37 (2000).
- ²²J. Ryden, B. Hjörvarsson, T. Ericsson, E. Karlsson, A. Krozer, and B. Kasemo, *J. Less-Common Met.* **152**, 295 (1989).
- ²³P. Spatz, H. A. Aebischer, A. Krozer, and L. Schlappbach, *Z. Phys. Chem. (Munich)* **181**, 393 (1993).
- ²⁴F. G. Eisenberg, D. A. Zagnoli, and J. J. Sheridan, *J. Less-Common Met.* **74**, 323 (1980).
- ²⁵F. Stillesjö, S. Olafsson, B. Hjörvarsson, and E. Karlsson, *Z. Phys. Chem. (Munich)* **181**, 353 (1993).
- ²⁶P. Hjort, A. Krozer, and B. Kasemo, *J. Alloys Compd.* **237**, 74 (1996).
- ²⁷K. Higuchi, H. Kajioka, K. Toiyama, H. Fujii, S. Orimo, and Y. Kikuchi, *J. Alloys Compd.* **293–295**, 484 (1999).